

# In Situ Characterization of Photopolymerizable Systems Using a Thin-Film Calorimeter

Todd M. Roper,<sup>†</sup> Tai Yeon Lee,<sup>†</sup> C. Allan Guymon,<sup>‡</sup> and Charles E. Hoyle<sup>\*,†</sup>

Department of Polymer Science and Engineering, University of Southern Mississippi, Hattiesburg, Mississippi 39406, and Department of Chemical & Biochemical Engineering, University of Iowa, Iowa City, Iowa 52242

Received July 20, 2005; Revised Manuscript Received September 14, 2005

**ABSTRACT:** A thin-film calorimeter (TFC) was used to provide quantitative characterization of photopolymerizable systems. Photopolymerization exotherms measured using the TFC are compared with real-time infrared (RTIR) spectroscopic results. The TFC successfully monitored the in-situ polymerization kinetics of thin/thick films because of its increased sensitivity/resolution over traditional calorimetric instrumentation. Reproducible polymerization exotherms of trimethylolpropane triacrylate were measured on films as thin as 163 nm. Flexibility in the sample cell construction enables the characterization of both volatile reactants (closed cell) and the effect of oxygen inhibition (open cell). Several molecular systems were evaluated. First, exotherms for the reaction of a series of volatile hexene monomers with monofunctional thiol illustrate the effect of ene location on alkene reactivity. Second, vinyl acrylate, a volatile difunctional monomer with a unique polymerization mechanism, was shown to homopolymerize significantly faster than either of its monofunctional analogues. Additionally, the rapid instrument response time of the TFC allowed qualitative analysis of non-steady-state polymerization kinetics of vinyl acrylate.

## Introduction

Photopolymerization is a field undergoing significant growth because it is an efficient, energy-saving, economical, and environmentally friendly alternative to traditional solvent-based technology.<sup>1,2</sup> Specific areas of interest include the development and/or examination of ultrafast polymerizing monomers,<sup>3–8</sup> thin pigmented inks,<sup>9–11</sup> and thiol–enes.<sup>12–18</sup> Advances in instrumentation to characterize photopolymerization of these systems are necessary. The development of instrumentation with high sensitivities/resolution, rapid response times, and application flexibility is requisite and necessary for future technological advances in photopolymerization.

Chain growth polymerizations that involve the linking of small molecule building blocks (monomers) into large macromolecular chains (polymer) via a propagating free radical or ion are exothermic reactions; i.e., heat is released as double bonds are converted into single bonds.<sup>19</sup> Photoinduced polymerizations use high-energy radiation to generate free radicals or cations which initiate polymerization. Calorimetry, which measures the heat resulting from a physical or chemical change, is often used to monitor polymerizations.<sup>20</sup> The most commonly used photocalorimetric instrument is the photo-differential scanning calorimeter (photo-DSC). A photo-DSC measures the rate of heat evolution during polymerization against a reference. The photo-DSC, which is readily constructed from a standard DSC by fitting the DSC head with quartz windows above the sample and reference cells, has been successfully used to measure polymerization rates and non-steady-state kinetics.<sup>21–26</sup> Despite the widespread use of the photo-

DSC, limitations associated with the instrument prevent its ability to characterize numerous photopolymerization applications. Poor sensitivity and the dependence on large sample quantities prevent analysis of thin films, and slow instrument response times prevent the non-steady-state examination of many systems.

The first documented construction of a thin-film calorimeter for analysis of photocurable films was based upon a thin-foil copper–constantan thermocouple disclosed in a 1979 patent.<sup>27</sup> The calorimeter was used successfully to evaluate a novel photoinitiating composition consisting of peroxide(s) and a naphthalenic sensitizer by recording the thermocouple response as a function of irradiation time. Wisnosky and Fantazier described the subsequent construction of single cell calorimeter based on a thin-film heat flux sensor consisting of copper–constantan thermocouples connected in series.<sup>28</sup> The instrument was capable of monitoring photopolymerizations on films having a thickness between 100 and 250  $\mu\text{m}$  and produced data comparable to the photo-DSC. Hoyle et al. used the single-cell photocalorimeter to examine pulsed laser initiated thiol–ene polymerization kinetics.<sup>29</sup> Few published reports detailing modifications and/or applications of this technology to radiation curable systems have since appeared.<sup>30,31</sup> While these first-generation thin-film photocalorimeters were clearly shown to be a viable alternative to photo-DSC, they were limited in their ability to accurately measure ultrathin-film (<100  $\mu\text{m}$ ) polymerization exotherms due to deficient sensor sensitivity and poor detector resolution.

In an effort to develop a rapid method for the accurate evaluation of photopolymerization rate, extent of reaction, and ultimately the kinetics, a second-generation thin-film calorimeter (TFC) was constructed and optimized. The TFC has a flexible design; as a consequence, modifications can be easily made to tailor the instrument for evaluation of a wide variety of photopolymer-

<sup>†</sup> University of Southern Mississippi.

<sup>‡</sup> University of Iowa.

\* To whom correspondence should be addressed: e-mail charles.hoyle@usm.edu; Ph 601-266-4873; Fax 601-266-5504.

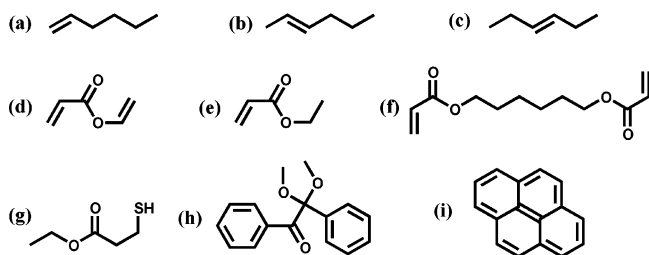


**Figure 1.** Chemical structures of (a) 1-hexene, (b) *trans*-2-hexene, (c) *trans*-3-hexene, (d) vinyl acrylate, (e) ethyl acrylate, (f) 1,6-hexanediol diacrylate (HDDA), (g) ethyl-3-mercaptopropionate (E3M), (h) 2,2-dimethoxy-2-phenylacetophenone (DMPA), and (i) pyrene.

ization processes. To emphasize the TFC's versatility, analysis of a variety of systems will be highlighted, including thin/thick acrylic films, thiol-enes, vinyl acrylate, and non-steady-state polymerization profiles. Where possible, real-time infrared (RTIR) spectroscopy will be used to confirm results of the photopolymerization exotherms measured using the TFC.

## Experimental Section

**Materials.** Reagents used from Aldrich Chemical Co. include 1-hexene, *trans*-2-hexene, *trans*-3-hexene, vinyl acrylate, ethyl acrylate, and ethyl 3-mercaptopropionate (E3M). UCB Chemicals Corp. supplied hexanediol diacrylate (HDDA) and trimethylolpropane triacrylate (TMPTA). The photoinitiator 2,2-dimethoxy-2-phenylacetophenone (DMPA) and an acylphosphine oxide blend (Darocur 4265) were provided by Ciba Specialty Chemicals. Pyrene was obtained from Sigma Chemical Co. All chemicals were used as received without additional purification, and their respective chemical structures are shown in Figure 1.

**Methods.** A Bruker IFS 88 modified to accommodate a horizontal sample accessory was used to collect real-time infrared (RTIR) spectroscopic data of photoreactions and photopolymerizations. Ultraviolet light from an Oriel lamp system (model 66057) equipped with a 200 W high-pressure mercury xenon bulb was channeled through an electric shutter, a 365 nm band-pass filter, and fiber optics into the sample chamber. Photoreactions were conducted by sandwiching the sample between two sodium chloride salt plates at a thickness of  $\sim 20\ \mu\text{m}$ . The salt plate edges were sealed with vacuum grease to suppress monomer evaporation, and samples were purged 10 min in nitrogen prior to irradiation. Light intensities were measured by a calibrated radiometer from International Light (IL-1400). Infrared absorbance spectra were obtained under continuous UV irradiation at a scanning rate of 5 scans/s. All thiol-ene samples were prepared with stoichiometric amounts of functional groups and contained 1.0 wt % of the photoinitiator dimethoxyphenylacetophenone (DMPA) unless otherwise noted. The characteristic IR absorbance bands used to monitor the disappearance of reactant/monomer during the photoreactions were as follows: terminal ene ( $1640$  and/or  $910\ \text{cm}^{-1}$ ), internal *trans* ene ( $968\ \text{cm}^{-1}$ ), acrylate ( $812\ \text{cm}^{-1}$ ), vinyl ester ( $1626\ \text{cm}^{-1}$ ), and thiol ( $2572\ \text{cm}^{-1}$ ).

UV-vis spectra were measured using a Cary 500 UV-vis-NIR spectrophotometer. The extinction coefficient of pyrene at  $338\ \text{nm}$  was measured to be  $33\,475\ \text{L mol}^{-1}\ \text{cm}^{-1}$ . Film thicknesses were determined by measuring the absorbance of the films with a known concentration of pyrene.

The general design of the thin-film calorimeter (TFC) is illustrated in Figure 2. The construction and signal optimization have been previously described in great detail.<sup>32-34</sup> An advanced thin-film heat flux sensor (Omega Engineering Inc.), consisting of 40 measurement sites connected in series, serves as the primary component of the TFC. The sensor is attached via double-sided thermally conductive tape onto a machined aluminum heat sink. Samples are prepared directly on the sensor surface in a variety of different configurations depend-

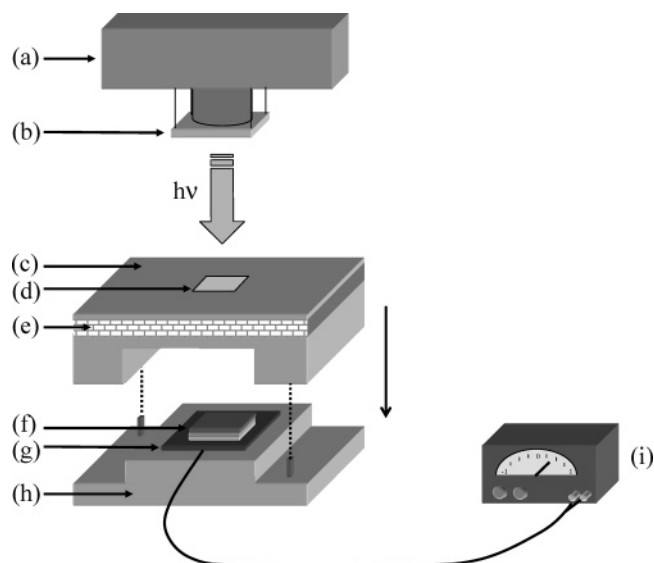


**Figure 2.** A diagram of the TFC: (a) lamp system, (b) electric shutter, (c) quartz heat shield, (d) 1 square cm opening in the machined aluminum lid, (e) insulating cork, (f) sample stack, (g) thin-film heat flux sensor, (h) machined aluminum heat sink, and (i) dc microvoltmeter.

ing on the application. In all cases, a protective substrate must be placed between the sample and sensor to prevent sensor damage. Protective substrates which are used include metal foil or glass coverslip. A small amount of conductive paste may be applied between the sensor and the protective substrate to ensure the intimate contact necessary for rapid and efficient heat transfer. Sample thickness is controlled by spin-coating (Chemat Technology spin-coater KW-4A) or dispersing a small quantity of spherical silica spacers (Emerson Cuming) of a specified diameter. After depositing the sample on the protective substrate, a glass/quartz coverslip or piece of transparent polyethylene film can be placed on top of the sample to prevent oxygen diffusion into the sample. Adjustable clamps (not pictured in Figure 2) press an aluminum cap, with a  $1\ \text{cm}^2$  hole machined through its center, onto the heat sink to ensure intimate contact throughout the sample configuration stack, therefore guaranteeing a uniform thickness. A 450 W medium-pressure mercury arc lamp (Ace Glass) equipped with an electric shutter is positioned above the sensor to serve as the UV light source. The sensor is connected to a battery-powered dc microvoltmeter (Keithley model 155). The voltmeter is interfaced with a PC through a multichannel A/D converter having 16 bit resolution and a maximum sampling rate of  $100\ \text{kHz}$ . A conversion factor of  $76.4\ \text{mW/mV}$  was used to convert the raw signal from the TFC to mW. The conversion factor was determined by calibration of TFC exotherms against photo-DSC results for identical samples irradiated under identical conditions as reported previously. A fully automated version of the TFC system is available from UV Process Supply.

## Results and Discussion

The TFC records polymerization exotherms by measuring the heat released as a function of time. Valuable information regarding the polymerization process, such as rate and extent of conversion, can be obtained from the polymerization exotherm. As an example, Figure 3 shows the photopolymerization exotherm from a  $100\ \mu\text{m}$  thick 1,6-hexanediol diacrylate (HDDA) sample with 1 wt % 1,1-dimethoxyphenylacetophenone (DMPA) photoinitiator. Upon irradiation, there is a brief inhibition period due to the presence of dissolved oxygen inhibiting the polymerization or impurities. The polymerization exotherm values are proportional to the polymerization rate at each point during the reaction, with the exo-

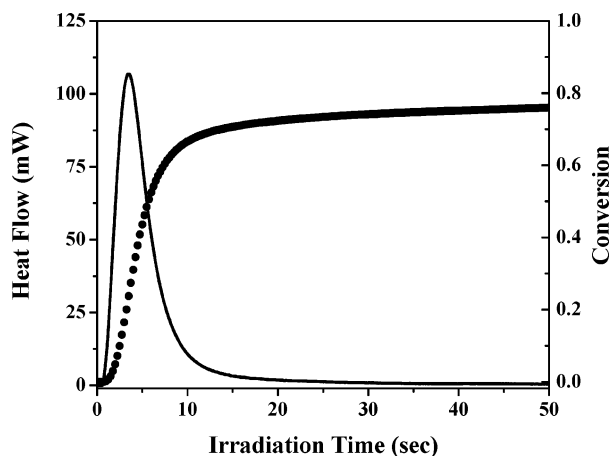


**Figure 3.** TFC photopolymerization exotherm (solid line) and conversion plot (●) of a 100  $\mu\text{m}$  thick HDDA sample with 1 wt % DMPA. Sample was polymerized using a 10  $\text{mW}/\text{cm}^2$  medium-pressure mercury light source.

therm maximum being proportional to the maximum polymerization rate. The area under the exotherm is equivalent to the total amount of heat released during polymerization. Considering the total amount of heat that would be released from a sample using the heat of polymerization for acrylates ( $\sim 80.4$   $\text{kJ}/\text{mol}$ ) and the quantity of sample being irradiated, the conversion at any time can be calculated. The resultant TFC conversion vs time plot for the HDDA sample in Figure 3 was determined to ultimately reach only 76%. Incomplete conversion is expected since HDDA is a difunctional acrylate which forms a cross-linked network during polymerization, resulting in unreacted acrylate groups being trapped.<sup>35–39</sup> With this brief introduction to the ability of the TFC in measuring photoinduced polymerization exotherms, we will describe in the next few sections the use of TFC for measuring photopolymerization profiles for several representative systems.

**I. Light Intensity and Sample Thickness in Acrylate Systems.** The TFC was designed to be extremely flexible with respect to experimental configuration and the variety of different experiments possible to perform. Photopolymerization kinetics can be measured for samples at various thicknesses and cure rates. To illustrate the ability of the TFC to characterize samples of different polymerization rates, HDDA photopolymerization exotherms were measured at various light intensities, as shown in Figure 4A. Neutral density filters from Omega Optical were used to uniformly attenuate the intensity of light. The exotherm shape significantly changes as the light intensity was decreased. The inhibition time and exotherm breadth both increase, while the exotherm maximum value decreases, all indications of a reduction in polymerization rate. As would be expected, the maximum exotherm values are also proportional to the light intensity to approximately the one-half power for HDDA samples having a thickness of 200  $\mu\text{m}$  and over the range of light intensities examined (0.2–20  $\text{mW}/\text{cm}^2$ ). The polymerization exotherm is also dependent on the film thickness as shown in Figure 4B. As film thickness decreases, the quantity of reactive groups within the 1  $\text{cm}^2$  irradiation window also decreases, reducing the total amount of heat released during the polymerization. As a result, the magnitude of the polymerization exotherms decreases as film thickness decreases. As can be seen from the results in Figure 4, the range for measuring accurate

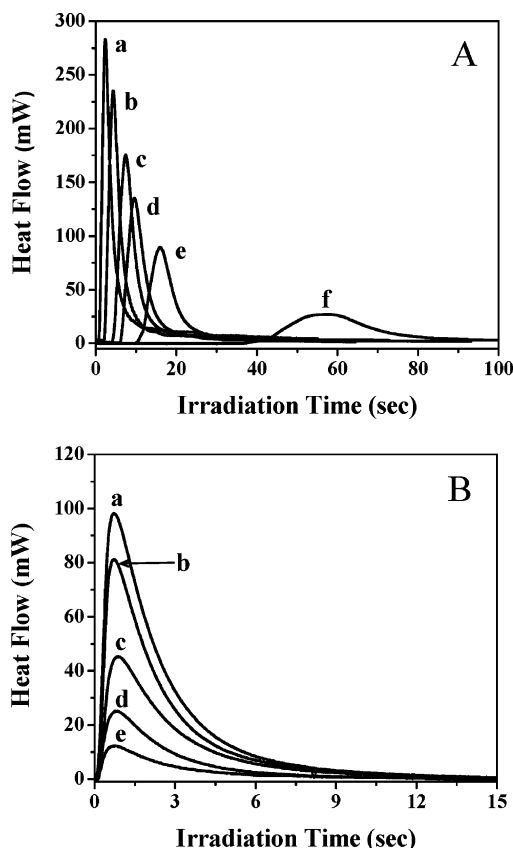


**Figure 4.** TFC photopolymerization exotherms of (A) 200  $\mu\text{m}$  thick HDDA samples with 1 wt % DMPA at a light intensity of (a) 23.7, (b) 8.0, (c) 3.8, (d) 2.7, (e) 1.3, and (f) 0.2  $\text{mW}/\text{cm}^2$  and (B) TFC photopolymerization exotherms of HDDA samples with 1 wt % DMPA polymerized using a medium-pressure mercury lamp with an intensity of 20  $\text{mW}/\text{cm}^2$  at sample thicknesses of (a) 25, (b) 20, (c) 15, (d) 10, and (e) 5  $\mu\text{m}$ .

exotherms directly for the TFC thus extends from 200 to 5  $\mu\text{m}$ , 2 orders of magnitude. We point out that the ability to measure exotherm polymerization kinetics for a wide range of thicknesses is indeed unique to TFC, virtually impossible to accomplish using photo-DSC. In addition, monitoring over such a wide range of thicknesses is difficult to accomplish using RTIR. The absorbance of reactive groups at low concentrations (thin films) cannot be accurately detected, and the difficulty in obtaining accurate results for thicker samples, where functional group absorbances are very high, is due to a nonlinear correlation between functional group concentration and absorbance.

It is possible to extend the range of the TFC unit to measure considerably smaller exotherms that arise from polymerizing samples that are significantly less than 5  $\mu\text{m}$  by recording both the direct exotherm and the background heat flow that results from absorption of the lamp output by the combination of the polymerized sample and the sample pan. To illustrate exactly how sensitive the TFC is when operated in this mode, the exotherms of ultrathin films on the submicron size scale were measured. Films were prepared by spin-coating trimethylolpropane triacrylate (TMPTA) containing 3 wt % Darocur 4265 photoinitiator onto glass coverslips. The mixture also contained a 0.24 M concentration of pyrene, thus allowing the measurement of film thickness of such thin films using a UV–vis spectrometer. As shown in Figure 5, polymerization exotherms of films as thin as 163 nm can be measured by this technique,



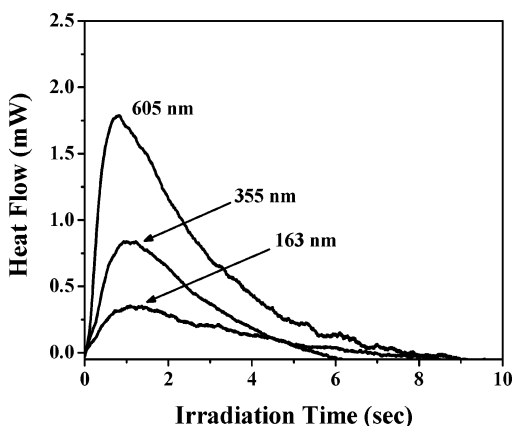


**Figure 5.** TFC photopolymerization exotherms of 605, 355, and 163 nm TMPTA films with 3 wt % Darocur 4265 using the unfiltered 65 mW/cm<sup>2</sup> output of a medium-pressure mercury lamp.

i.e., by subtracting the background heat from the initial convoluted polymerization exotherm. Not only do the exotherms increase in value as the sample thickness is increased to 355 and 605 nm, but the curves results are also reproducible. The curves in Figure 5 are the first documented photopolymerization exotherms of a sub-micron thick sample; indeed, it is very difficult to obtain real-time conversion of monomer polymerization for such thin films using any technique. Thus, we have shown that the TFC unit is able to record exotherms for samples with thicknesses over 3 orders of magnitude. In the future, we expect to extend this range to cover samples greater than 200  $\mu$ m and less than 100 nm.

## II. Thiol–Ene Photoinitiated Polymerizations.

Thiol–ene photopolymerization has been extensively studied since the mid-1970s due to advantages with respect to both the polymerization process and film properties.<sup>40–42</sup> Thiol–ene reactions are free radical in nature and follow a two-step chain reaction: thiyl radical insertion in the ene, followed by a chain transfer hydrogen abstraction reaction from another thiol to regenerate the thiyl radical. The thiol–ene reaction is extremely versatile because it copolymerizes with virtually any ene, both electron rich and electron poor. Thiol–ene photoreactions involving simple alkenes have proven difficult to study using traditional calorimetric instruments due to their volatility. Since the sample volatility can be eliminated by using a coverslip, the TFC is able to successfully characterize such systems. Figure 6A,B shows the photoreaction exotherms and the corresponding percent conversion vs time plots for the reaction of a series of hexene monomers with the monofunctional thiol, ethyl-3-mercaptopropionate (E3M), measured using the TFC. 1-Hexene, which is a monosubstituted terminal ene, has a significantly higher reactivity than the disubstituted internal enes, 2-hexene and 3-hexene. In fact, the maximum of the reaction exotherm (Figure 6A) is more than 10 times greater than 2-hexene and 18 times greater than 3-hexene. As indicated in Figure 6B, complete conversion for the 1-hexene system is reached in  $\sim$ 40 s, with the thiol–ene mixtures involving the internal enes, 2-hexene and 3-hexene, reaching only 80% and 55% conversions, respectively, during the same time period. The difference in reactivity has been reported to be due to a reduction in the rate of chain transfer hydrogen abstraction reaction in the thiol–ene reaction sequence caused by enhanced steric hindrance.<sup>43</sup> The corresponding RTIR data of ene conver-

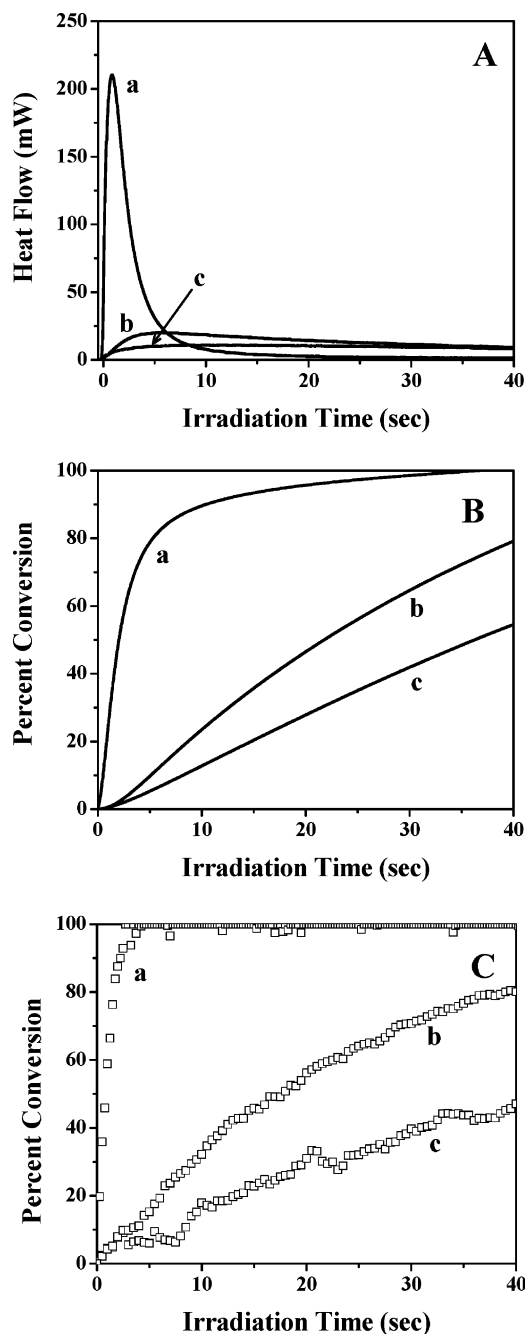


**Figure 6.** (A) TFC photopolymerization exotherms of 200  $\mu$ m thick samples of 50/50 molar alkene/E3M mixtures, (B) TFC-based percent conversion vs time plots based on these exotherms, and (C) RTIR alkene conversion vs time plots and for (a) 1-hexene, (b) *trans*-2-hexene, and (c) *trans*-3-hexene. Samples contain 1 wt % DMPA. Light intensity of the 365 nm monochromatic light was  $\sim$ 3.0 mW/cm<sup>2</sup>.

sion as a function of time shown in Figure 6C complement the results in Figure 6B obtained using the TFC. Both methods show remarkably consistent results. From the IR plots 1-hexene reacts significantly faster with E3M, reaching 100% conversion in less than 5 s, much faster than either 2-hexene or 3-hexene, which are not fully reacted after 40 s of irradiation. The initial slopes of the conversion vs time plots, which give the conversion rates, indicate that 1-hexene with a terminal ene is 13 and 25 times faster than *trans*-2-hexene and *trans*-3-hexene, respectively, very similar to the conversion rates given by the TFC. It is quite clear that the TFC is able to successfully monitor the photoreaction of thiol

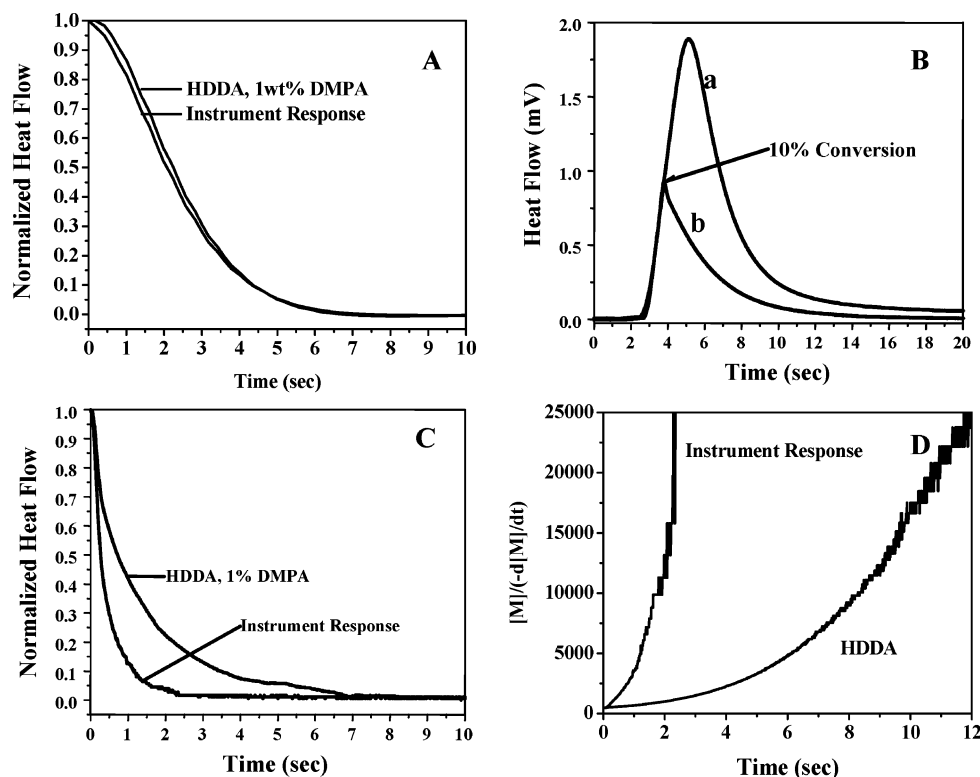


**Figure 7.** (A) Normalized photo-DSC decay curves for 200  $\mu\text{m}$  HDDA films exposed to the output of a medium-pressure mercury lamp with intensity of 17  $\text{mW}/\text{cm}^2$  for 2 s and the normalized instrument response decay. (B) TFC photopolymerization exotherms of 200  $\mu\text{m}$  thick HDDA films with 1 wt % DMPA exposed to the output of medium-pressure mercury lamp with light intensity of 17  $\text{mW}/\text{cm}^2$  (a) continuously and (b) for 2 s. (C) TFC normalized decay curve for the HDDA film in (B) exposed for 2 s and normalized instrument response function decay. (D) Plot of  $[M]/(-d[M]/dt)$  vs time from TFC for the HDDA film in (B) after exposure to the output of the medium-pressure mercury lamp for 2 s and plot of the reciprocal of the normalized instrument response function vs time.

with the volatile hexene reactants. This illustrates the utility of the TFC in measuring the polymerization exotherms of very volatile monomers.

**III. Non-Steady-State Exotherm Decays.** Until now, the thin-film calorimeter has been used to record exotherms of photopolymerizable acrylates during continuous exposure to a medium-pressure mercury lamp (steady-state conditions). It was shown in a report in the late 1970s that if the light is suddenly removed by closing the shutter between the sample and the lamp source, the exotherm will decay due to the predominance of the radical termination processes which effectively remove radicals from the medium.<sup>21</sup> Subsequent analysis of the non-steady-state polymerization rate measurements yield the ratio of the rate constants for termination and propagation. Combining rate constant ratios from non-steady-state experiments with steady-state experiments enables the direct calculation of propagation and termination rate constants. Unfortunately, because of the rather efficient process of termination at low acrylate conversions in the polymerization of multifunctional acrylates when the overall viscosity of the medium is relatively low, it was difficult (actually impossible) to obtain reasonable exotherm decay curves due to the long instrument response function of the DSC.<sup>21</sup> We will next illustrate the heart of the problem in obtaining exotherm decays for such systems at low conversion. Figure 7A shows the normalized exotherm decay from a traditional photo-DSC<sup>24</sup> for a HDDA sample terminated after low conversion (less than 10%) attained by shuttering the lamp after 2 s of continuous exposure to a medium-pressure mercury lamp. Also plotted is the decay of a normalized pure heat

signal obtained by exposing a totally absorbing black sample pan. The results in Figure 7A clearly illustrate the problem encountered when attempting to evaluate exotherm decays of multifunctional monomers when the light source is removed using photo-DSC; i.e., the exotherm decay is essentially dictated by the decay of the instrument response function, and separation of the true exotherm decay from the instrument decay cannot be successfully accomplished, even if a mathematical deconvolution process is attempted. An accurate exotherm decay curve can be obtained using the thin-film calorimeter with a thin, 10  $\mu\text{m}$  thick, aluminum foil where heat flow time from the polymerizing monomer across the thin-film heat flow detector to the heat sink is minimized. Figure 7B shows the exotherm (continuous exposure) of an HDDA sample exposed to the continuous output of a medium-pressure mercury lamp (curve a) and the exotherm of an identical HDDA sample where the light was terminated after attaining  $\sim 10\%$  conversion (curve b). The resultant normalized exotherm decay with time zero taken as the instant that the light was terminated is shown in Figure 7C along with the normalized decay of the instrument response function obtained by using a blackbody absorber. In contrast to the results in Figure 7A, the decay of the HDDA polymerization exotherm is clearly much longer than the decay of the thin-film instrument response function. Based on the HDDA exotherm decay in Figure 7C, a direct plot of the ratio of the monomer concentration,  $[M]$ , to the rate of monomer loss,  $-d[M]/dt$ , vs the time after removing the light source is shown in Figure 7D. This plot is suggested by the traditional equation<sup>21</sup> that is an attempt to describe the polymerization rate

decay upon removal of the initiating light source shown in eq 1.

$$\frac{[M]}{-d[M]/dt} = 2(k_t/k_p)t + \frac{([M])_0}{(-d[M]/dt)_0} \quad (1)$$

**IV. Vinyl Acrylate Photopolymerization.** Vinyl acrylate is an extremely interesting molecule because it is made up of two reactive groups having different reactivity: an acrylate double bond and a vinyl double bond. It has been previously shown that during the polymerization of vinyl acrylate the acrylate group homopolymerizes first followed by a slow reaction on the vinyl group. Figure 8A depicts the RTIR conversion vs time plots for homopolymerization of vinyl acrylate along with one of its monofunctional analogues, ethyl acrylate. The reactivity of ethyl acrylate is much less than that of the acrylate group in vinyl acrylate. Complementary calorimetric data via photo-DSC are not possible because of the volatility of vinyl acrylate. Since TFC can be used to measure the exotherms of volatile monomers, it should be possible to accurately obtain direct exotherms for vinyl acrylate. The TFC photopolymerization exotherms of vinyl acrylate and ethyl acrylate are shown in Figure 8B. To allow more direct comparison of the IR conversion data, a normalized conversion was also found from the exotherms by integrating the area under the curve. As the conversion cannot be directly calculated from the exotherm due to the presence of both acrylate and vinyl groups, the normalized conversion is based simply on the fraction of total heat released during polymerization. The corresponding normalized conversions as a function of polymerization time are shown in Figure 8C. Vinyl acrylate is clearly much more reactive than the monofunctional analogue, ethyl acrylate. Both the curve shapes and the rate of conversion appear to be essentially identical to the plots obtained using RTIR (Figure 8A), even with the proviso that the normalized percent conversion is only an approximation for conversion. Such excellent agreement with IR results further validates the accuracy and sensitivity of TFC in examining photopolymerization kinetics.

As previously discussed, vinyl acrylate is unique in that its polymerization mechanism essentially consists of two processes: acrylate homopolymerization followed by cross-linking through vinyl polymerization. This two-part mechanism results in autoacceleration or an increase in the polymerization rate at the gel point. The increase in rate upon gelation can be further explained by comparing the rate at which polymerization exotherms decay to the baseline at various stages of the polymerization. Figure 9A shows the full vinyl acrylate photopolymerization exotherm and exotherms produced when the light has been removed at various points during the polymerization. In an effort to examine the effect of gelation on the polymerization kinetics, decays were monitored after (a) 5%, (b) 30%, and (c) 80% vinyl acrylate conversion. Figure 9B,C directly compares the three normalized polymerization decays in terms of the normalized exotherm decay and the reciprocal of the normalized exotherm vs time. The decay to the baseline for the polymerization carried out to 5% conversion is fast, indicating a more rapid termination of the radicals compared to the decays starting after the onset of gelation has occurred (curves b and c). The difference in decay times for polymerizations carried out to 30%

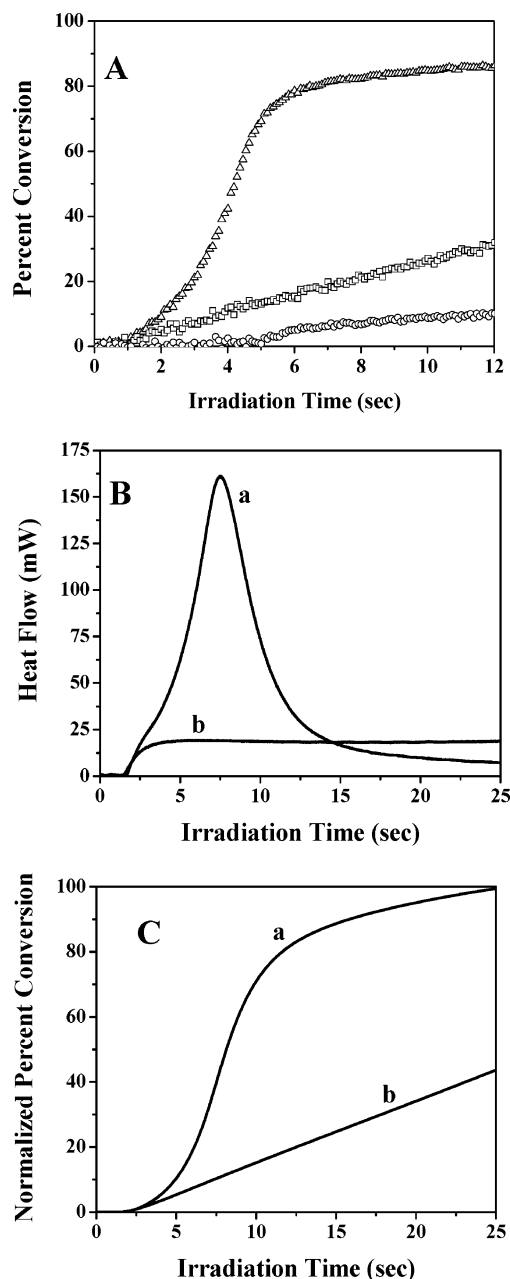


**Figure 8.** (A) RTIR conversion vs time plots for conversion of the acrylate ( $\Delta$ ) and vinyl ( $\circ$ ) groups of 25  $\mu\text{m}$  vinyl acrylate films and the acrylate group ( $\square$ ) of 25  $\mu\text{m}$  ethyl acrylate with 0.5 wt % DMPA and the isolated 365 nm line with intensity of 14  $\text{mW}/\text{cm}^2$  of a high-pressure mercury lamp. (B) TFC photopolymerization exotherms of 80  $\mu\text{m}$  (a) vinyl acrylate and (b) ethyl acrylate films with 0.5 wt % DMPA and the isolated 365 nm line with intensity of 14  $\text{mW}/\text{cm}^2$  of a medium-pressure mercury lamp. (C) Normalized percent conversion time plots of 80  $\mu\text{m}$  (a) vinyl acrylate and (b) ethyl acrylate films with 0.5 wt % DMPA using the isolated 365 nm line with intensity of 14  $\text{mW}/\text{cm}^2$  from a medium-pressure mercury lamp.

and 80% conversion suggests an increase in cross-link density throughout the polymerization causing radicals to be trapped in the polymer network,<sup>44</sup> resulting in a reduction in the rate of termination and a slower return to the baseline (a lower slope for plots b and c in Figure 9C than plot a). As pointed out earlier for the plot for HDDA in Figure 7D, a straight line is not attained for acrylate polymerization due to multiple rate constants not taken into account in eq 1. Finally, we note the reproducibility of TFC exotherms as again demonstrated in Figure 9A. The four vinyl acrylate polymerizations

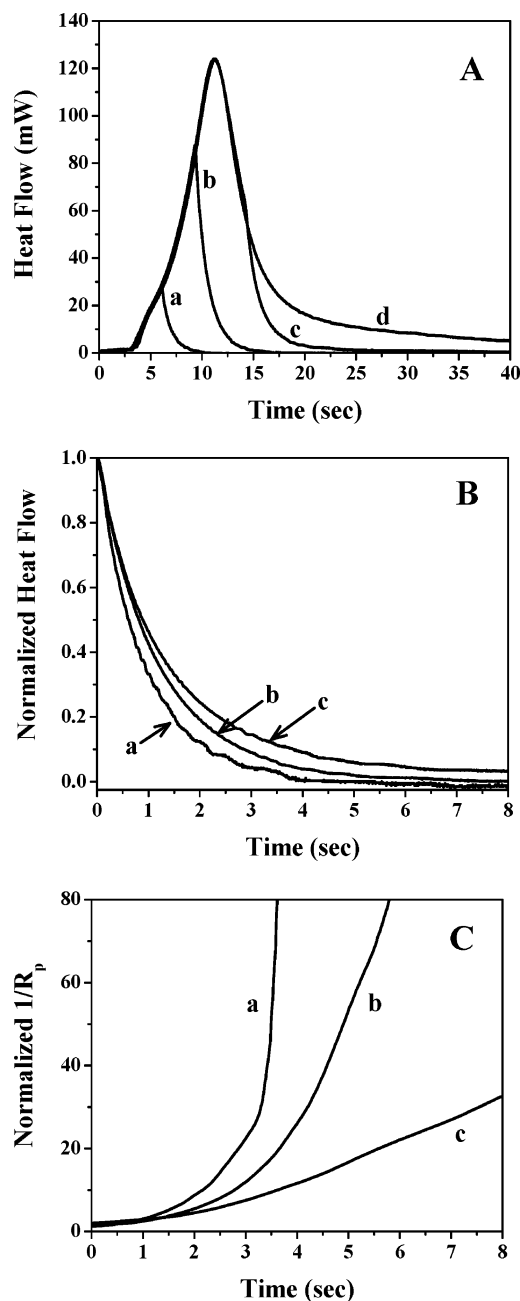


**Figure 9.** (A) TFC photopolymerization exotherms of 100  $\mu\text{m}$  thick vinyl acrylate samples containing 1 wt% DMPA. Light having an intensity of 40  $\text{mW}/\text{cm}^2$  was removed after reaching (a) 5%, (b) 30%, (c) 80%, and (d) maximum conversion of vinyl acrylate. (B) Normalized decay curves for the vinyl acrylate samples polymerized to a conversion of (a) 5%, (b) 30%, and (c) 80%. (C) Plots of  $[M]/(-d[M]/dt)$  vs time for vinyl acrylate polymerized to (a) 5%, (b) 30%, and (c) 80% vinyl acrylate conversion.

measured follow almost identical curves up to the point of terminating the light source, illustrating the exceptional reliability and reproducibility in examining photopolymerizations using TFC.

## Conclusions

A thin-film calorimeter (TFC) was used to characterize several photopolymerizable systems. Photopolymerization exotherms measured using the TFC are compared with real-time infrared (RTIR) spectroscopic results. The TFC is able to successfully monitor the in-situ polymerization kinetics of thin and thick films

because of increased sensitivity compared to traditional calorimetric instrumentation. Exotherms of samples with thicknesses that varied by over 3 orders of magnitude were successfully recorded. The polymerization exotherm of films as thin as 163 nm were accurately measured. The flexibility in construction of the sample cell enables the characterization of very volatile reactants. Reaction exotherms from a variety of volatile hexene monomers reacting with monofunctional thiol illustrate the effect of ene location on alkene reactivity. The rapid instrument response time of the TFC results in the ability to measure accurately non-steady-state exotherm decays of 1,6-hexanediol diacrylate at low conversions. Vinyl acrylate, a volatile monomer with a unique polymerization mechanism, was shown to homopolymerize significantly faster than either of its monofunctional acrylate analogues.

**Acknowledgment.** The authors of this paper thank Fusion UV Systems Inc. and the National Science Foundation (Tie Grant 0120943) in cooperation with the Industry/University Cooperative Research Center in Coatings (EEC 0002775) for funding of this research.

## References and Notes

- (1) Fouassier, J. P. *Photoinitiation Photopolymerization and Photocuring; Fundamentals and Applications*; Hanser Publishers: Munich, 1995.
- (2) Pappas, S. P. *Radiation Curing Science and Technology*; Plenum Press: New York, 1992.
- (3) Decker, C.; Moussa, K. *Makromol. Chem.* **1991**, *192*, 507.
- (4) Decker, C.; Moussa, K. *Eur. Polym. J.* **1991**, *27*, 881.
- (5) Moussa, K.; Decker, C. *J. Polym. Sci., Part A: Polym. Chem.* **1993**, *31*, 2197.
- (6) Lee, T. Y.; Roper, T. M.; Jonsson, S. E.; Kudyakov, I.; Viswanathan, K.; Nason, C.; Guymon, C. A.; Hoyle, C. E. *Polymer* **2003**, *44*, 2.
- (7) Lee, T. Y.; Roper, T. M.; Jonsson, S. E.; Guymon, C. A.; Hoyle, C. E. *Macromolecules* **2003**, *37*, 3659.
- (8) Berchtold, K. A.; Nie, J.; Stansbury, J. W.; Hacıoglu, B.; Beckel, E. R.; Bowman, C. N. *Macromolecules* **2004**, *37*, 3165.
- (9) Roper, T. M.; Kwee, T.; Lee, T. Y.; Guymon, C. A.; Hoyle, C. E. *Polymer* **2004**, *45*, 2921.
- (10) Yang, B. *Radtech US 2000 Technical Proceedings*, p 271.
- (11) Roper, T. M.; Rhudy, K. L.; Chandler, C. M.; Guymon, C. A.; Hoyle, C. E. *Radtech US 2002 Technical Proceedings*, p 697.
- (12) Jacobine, A. F. In *Radiation Curing in Polymer Science and Technology III, Polymerization Mechanisms*; Fouassier, J. D., Rabek, J. F., Eds.; Elsevier Applied Science: London, 1993; p 219.
- (13) Lee, T. Y.; Roper, T. M.; Jonsson, S. E.; Guymon, C. A.; Hoyle, C. E. *Macromolecules* **2004**, *37*, 3606.
- (14) Chiou, B.; Khan, S. A. *Macromolecules* **1997**, *30*, 7322.
- (15) Natarajan, L. V.; Shepherd, C. K.; Brandelik, D. M.; Sutherland, R. L.; Chandra, S.; Tondiglia, V. P.; Tomlin, D.; Bunning, T. J. *Chem. Mater.* **2003**, *15*, 2477.
- (16) Cramer, N. B.; Scott, J. P.; Bowman, C. N. *Macromolecules* **2002**, *35*, 5361.
- (17) Cramer, N. B.; Bowman, C. N. *J. Polym. Sci., Part A: Polym. Chem.* **2001**, *39*, 3311.
- (18) Cramer, N. B.; Davies, T.; O'Brien, A. K.; Bowman, C. N. *Macromolecules* **2003**, *36*, 4631.
- (19) Odian, G. *Principles of Polymerization*, 3rd ed.; Wiley-Interscience: New York, 1991.
- (20) Hoyle, C. E. In *Radiation Curing Science and Technology*; Pappas, S. P., Ed.; Plenum Press: New York, 1992; p 57.
- (21) Tryson, G. R.; Shultz, A. R. *J. Polym. Sci., Polym. Phys. Ed.* **1979**, *17*, 2059.
- (22) Crivello, J. V.; Lam, J. H. W. *J. Polym. Sci., Polym. Chem. Ed.* **1979**, *17*, 1059.
- (23) Guymon, C. A.; Hoggan, E. N.; Clark, N. A.; Rieker, T. P.; Walba, D. M.; Bowman, C. N. *Science* **1997**, *275*, 57.
- (24) Guymon, C. A.; Bowman, C. N. *Macromolecules* **1997**, *30*, 5271.
- (25) Kloosterboer, J. G.; Lijten, G. F. C. M. *Polym. Commun.* **1987**, *28*, 2.



- (26) Anseth, K. S.; Bowman, C. N.; Nelson, E. W.; Jacobs, J. L.; Scranton, A. B. *Polymer* **1995**, *36*, 4651.
- (27) Fantazier, R. M. US Patent #4,171,252 1979.
- (28) Wisnosky, J. D.; Fantazier, R. M. *J. Radiat. Curing* **1981**, *8*, 16.
- (29) Hoyle, C. E.; Hensel, R. D.; Grubb, M. B. *Polym. Photochem.* **1984**, *4*, 69.
- (30) Pargellis, A. N. *Rev. Sci. Instrum.* **1986**, *57*, 1384.
- (31) Hager, N. E., Jr. *Rev. Sci. Instrum.* **1987**, *58*, 86.
- (32) Roper, T. M.; Guymon, C. A.; Hoyle, C. E. *Radtech US 2004 Technical Proceedings*.
- (33) Roper, T. M.; Guymon, C. A.; Hoyle, C. E. *Polym. Mater. Sci. Eng.* **2003**, *88*, 219.
- (34) Roper, T. M.; Guymon, C. A.; Hoyle, C. E. *Rev. Sci. Instrum.* **2005**, *76*, 054102.
- (35) Kloosterboer, J. G.; van de hei, G. M. M.; Gossink, R. G.; Dortant, G. C. M. *Polym. Commun.* **1984**, *25*, 322.
- (36) Boots, H. M. J.; Kloosterboer, J. G.; van de hei, G. M. M. *Br. Polym. J.* **1985**, *17*, 219.
- (37) Kloosterboer, J. G.; van de hei, G. M. M.; Boots, H. M. J. *Polym. Commun.* **1984**, *25*, 354.
- (38) Kloosterboer, J. G.; Lijten, G. F. C. M. *Makromol. Chem., Macromol. Symp.* **1989**, *24*, 223.
- (39) Kloosterboer, J. G.; van de hei, G. M. M.; Lijten, G. F. C. M. *Integration of Fundamental Polymer Science and Technology*; Elsevier Applied Science: London, 1987; pp 198–203.
- (40) Morgan, C. R.; Ketley, A. D. *J. Radiat. Curing* **1980**, *10*.
- (41) Morgan, C. R.; Ketley, A. D. *J. Polym. Sci., Polym. Chem. Ed.* **1977**, *15*, 627.
- (42) Morgan, C. R.; Magnotta, F.; Ketley, A. D. *J. Polym. Sci., Polym. Chem. Ed.* **1977**, *15*, 627.
- (43) Roper, T. M.; Guymon, C. A.; Jonsson, E. S.; Hoyle, C. E. *J. Polym. Sci., Part A: Polym. Chem.* **2004**, *42*, 6283.
- (44) Kloosterboer, J. G.; Lijten, G. F. C. M.; Greidanus, F. J. A. M. *Polym. Commun.* **1986**, *27*, 268.

MA051586I